

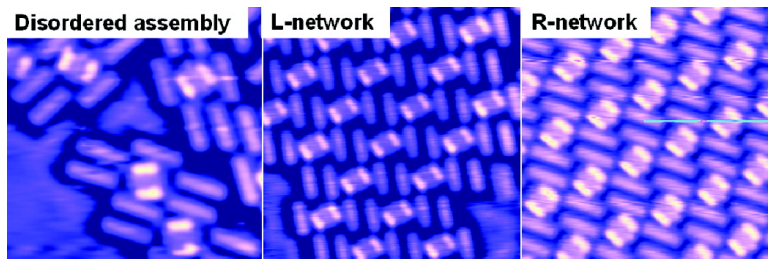
Article

## Two-Dimensional Pentacene:3,4,9,10-Perylenetetracarboxylic Dianhydride Supramolecular Chiral Networks on Ag(111)

Wei Chen, Hui Li, Han Huang, Yuanxi Fu, Hong Liang Zhang, Jing Ma, and Andrew Thye Shen Wee

*J. Am. Chem. Soc.*, 2008, 130 (37), 12285-12289 • DOI: 10.1021/ja801577z • Publication Date (Web): 23 August 2008

Downloaded from <http://pubs.acs.org> on February 8, 2009



### More About This Article

Additional resources and features associated with this article are available within the HTML version:

- Supporting Information
- Access to high resolution figures
- Links to articles and content related to this article
- Copyright permission to reproduce figures and/or text from this article

[View the Full Text HTML](#)

## Two-Dimensional Pentacene:3,4,9,10-Perylenetetracarboxylic Dianhydride Supramolecular Chiral Networks on Ag(111)

Wei Chen,<sup>\*,†</sup> Hui Li,<sup>‡</sup> Han Huang,<sup>†</sup> Yuanxi Fu,<sup>‡</sup> Hong Liang Zhang,<sup>†</sup> Jing Ma,<sup>\*,‡</sup> and Andrew Thye Shen Wee<sup>\*,†</sup>

*Department of Physics, National University of Singapore, 2 Science Drive 3, 117542 Singapore, and Institute of Theoretical and Computational Chemistry, Department of Chemistry, Nanjing University, Hankou Road 22, Nanjing, 210093 P.R. China*

Received March 3, 2008; E-mail: phycw@nus.edu.sg (W.C.); majing@netra.nju.edu.cn (J.M.); phyweets@nus.edu.sg (A.T.S.W.)

**Abstract:** Self-assembly of the binary molecular system of pentacene and 3,4,9,10-perylenetetracarboxylic dianhydride (PTCDA) on Ag(111) has been investigated by low-temperature scanning tunneling microscopy, molecular dynamics (MD), and density functional theory (DFT) calculations. Well-ordered two-dimensional (2D) pentacene:PTCDA supramolecular chiral networks are observed to form on Ag(111). The 2D chiral network formation is controlled by the strong interfacial interaction between adsorbed molecules and the underlying Ag(111), as revealed by MD and DFT calculations. The registry effect locks the adsorbed pentacene and PTCDA molecules into specific adsorption sites due to the corrugation of the potential energy surface. The 2D supramolecular networks are further constrained through the directional C=O···H—C multiple intermolecular hydrogen bonding between the anhydride groups of PTCDA and the peripheral aromatic hydrogen atoms of the neighboring pentacene molecules.

### Introduction

Self-assembled molecular superstructures with well-defined orientation, conformation, and two-dimensional (2D) organization on surfaces have potential applications in organic<sup>1</sup> and molecular electronics<sup>2</sup> and biosensors.<sup>3</sup> In particular, the development of molecular nanodevices relies on the controlled positioning and assembly of functional molecules on surfaces, which crucially depends on the interplay between various chemical and physical bonds formed and lateral interactions of different strength and length scales.<sup>4</sup> Directional intermolecular interactions, such as hydrogen-bonding (H-bonding) and metal–ligand interactions, have been widely used in supramo-

lecular chemistry to fabricate engineered molecular crystals and, more recently, surface-supported one-dimensional (1D) or 2D highly periodic supramolecular assemblies, including molecular supergrating,<sup>5</sup> honeycomb networks,<sup>6</sup> and various rationally designed molecular nanostructures.<sup>7–9</sup> In some cases, molecular self-assembly on surfaces can lead to the formation of chiral supramolecular structures.<sup>12</sup> Such chiral effects can arise from the adsorption of chiral molecules on substrates, where the chirality of the adsorbates is transferred to the surface assemblies,<sup>13</sup> or the adsorption on the high-index chiral metal

<sup>†</sup> National University of Singapore.

<sup>‡</sup> Nanjing University.

- (1) (a) Dimitrakopoulos, C. D.; Malenfant, P. R. L. *Adv. Mater.* **2002**, *14*, 99. (b) Coropceanu, V.; J.; Cornil, J.; da Silva, D. A.; Olivier, Y.; Silbey, R.; Bredas, J. L. *Chem. Rev.* **2007**, *107*, 926.
- (2) (a) Joachim, C.; Ratner, M. A. *Proc. Natl. Acad. Sci. U.S.A.* **2005**, *102*, 8801. (b) Heath, J. H.; Ratner, M. A. *Phys. Today* **2003**, *56*, 43. (c) Joachim, C.; Gimzewski, J. K.; Aviram, A. *Nature* **2000**, *408*, 541.
- (3) (a) Park, T. J.; Lee, S. Y.; Lee, S. J.; Park, J. P.; Yang, K. S.; Lee, K.-B.; Ko, S.; Park, J. B.; Kim, T.; Kim, S. K.; Shin, Y. B.; Chung, B. H.; Ku, S.-J.; Kim, D. H.; Choi, I. S. *Anal. Chem.* **2006**, *78*, 7197. (b) Rosi, N. L.; Mirkin, C. A. *Chem. Rev.* **2005**, *105*, 1547. (c) Smith, J. C.; Lee, K.-B.; Wang, Q.; Finn, M. G.; Johnson, J. E.; Mrksich, M.; Mirkin, C. A. *Nano Lett.* **2003**, *3*, 883.
- (4) (a) Barth, J. V.; Constantini, G.; Kern, K. *Nature* **2005**, *437*, 671. (b) Rosei, F. J. *Phys.: Condens. Matter* **2004**, *16*, S1373. (c) Chen, W.; Wee, A. T. S. *J. Phys. D: Appl. Phys.* **2007**, *40*, 6287. (d) Tao, F.; Bernasek, S. L. *Chem. Rev.* **2007**, *107*, 1408. (e) Rosei, F.; Schunack, M.; Naitoh, Y.; Jiang, P.; Gourdon, A.; Laegsgaard, E.; Stensgaard, I.; Joachim, C.; Besenbacher, F. *Prog. Surf. Sci.* **2003**, *71*, 95. (f) Yuan, L. F.; Yang, J. L.; Wang, H. Q.; Zeng, C. G.; Li, Q. X.; Wang, B.; Hou, J. G.; Zhu, Q. S.; Chen, D. M. *J. Am. Chem. Soc.* **2003**, *125*, 169. (g) Hou, J. G.; Yang, J. L.; Wang, H. Q.; Li, Q. X.; Zeng, C. G.; Yuan, L. F.; Wang, B.; Chen, D. M.; Zhu, Q. S. *Nature* **2001**, *409*, 304.

- (5) (a) Weckesser, J.; De Vita, A.; Barth, J. V.; Cai, C.-Z.; Kern, K. *Phys. Rev. Lett.* **2001**, *87*, 096101. (b) Barth, J. V.; Weckesser, J.; Cai, C.-Z.; Günter, P.; Bürgi, L.; Jeandupeux, O.; Kern, K. *Angew. Chem., Int. Ed.* **2000**, *39*, 1230. (c) Barth, J. V.; Weckesser, J.; Trimarchi, G.; Vladimirova, M.; De Vita, A.; Cai, C.-Z.; Brune, H.; Günter, P.; Kern, K. *J. Am. Chem. Soc.* **2002**, *124*, 7991. (d) Pawin, G.; Wong, K. L.; Kwon, K. Y.; Bartels, L. *Science* **2006**, *313*, 961. (e) Huang, T.; Hu, Z.; Zhao, A.; Wang, H.; Wang, B.; Yang, J. L.; Hou, J. G. *J. Am. Chem. Soc.* **2007**, *129*, 3857.
- (6) (a) Theobald, J. A.; Oxtoby, N. S.; Phillips, M. A.; Champness, N. R.; Beton, P. H. *Nature* **2003**, *424*, 1029. (b) Theobald, J. A.; Oxtoby, N. S.; Champness, N. R.; Beton, P. H.; Dennis, T. J. S. *Langmuir* **2005**, *21*, 2038. (c) Perdigão, L. M. A.; Perkins, E. W.; Ma, J.; Staniec, P. A.; Rogers, B. L.; Champness, N. R.; Beton, P. H. *J. Phys. Chem. B* **2006**, *110*, 12539. (d) Staniec, P. A.; Perdigão, L. M. A.; Saywell, A.; Champness, N. R.; Beton, P. H. *ChemPhysChem* **2007**, *8*, 2177.
- (7) (a) Yokoyama, T.; Yokoyama, S.; Kamikado, T.; Okuno, Y.; Mashiko, S. *Nature* **2001**, *413*, 619. (b) Perdigao, L. M. A.; Champness, N. R.; Beton, P. H. *Chem. Commun.* **2006**, 538. (c) Swarbrick, J. C.; Rogers, B. L.; Champness, N. R.; Beton, P. H. *J. Phys. Chem. B* **2006**, *110*, 6110. (d) Otero, R.; Schock, M.; Molina, L. M.; Laegsgaard, E.; Stensgaard, I.; Hammer, B.; Besenbacher, F. *Angew. Chem., Int. Ed.* **2005**, *44*, 2270. (e) Schnadt, J.; Rauls, E.; Xu, W.; Vang, R. T.; Knudsen, J.; Laegsgaard, E.; Li, Z.; Hammer, B.; Besenbacher, F. *Phys. Rev. Lett.* **2008**, *100*, 046103.
- (8) (a) Stepanow, S.; Lingenfelder, M.; Dmitriev, A.; Spillmann, H.; Delvigne, E.; Deng, X.; Cai, C.; Barth, J. V.; Kern, K. *Nat. Mater.* **2004**, *3*, 229. (b) Stepanow, S.; Lin, N.; Barth, J. V.; Kern, K. *Chem. Commun.* **2006**, 2153.

surfaces.<sup>14</sup> The assembly of symmetric molecules on surfaces can also induce surface chirality because 2D confinement removes mirror symmetry in the plane of the substrates.<sup>5a,15</sup> Examples include the highly directional 1D chiral chains of 4-[*trans*-2-(pyrid-4-vinyl)]benzoic acid (PVBA) on Ag(111)<sup>5a</sup> and short molecular rods of adenine on Cu(110),<sup>16</sup> molecular nanoclusters of 1-nitronaphthalene on reconstructed Au(111),<sup>17</sup> the supramolecular assembly stabilized by metal–ligand interactions between iron atoms and 1,3,5-tricarboxylic benzoic acid (TMA) on Cu(100),<sup>18</sup> and extended 2D chiral networks of tartaric acid on Cu(111),<sup>13a</sup> heptahelicene on Cu(111),<sup>19</sup> and so on.

Highly directional interactions, such as H-bonding and metal–ligand interactions, can easily lead to the formation of short-range ordered molecular assemblies or nanostructures such as dimers and trimers, with well-defined binding geometries and molecular conformations.<sup>5–9,20</sup> However, the creation of long-range ordered molecular networks usually requires strong molecule–substrate interfacial interactions via epitaxial or quasi-epitaxial interlocking with single crystalline substrates<sup>21</sup> or through substrate-mediated long-range intermolecular interac-

tions.<sup>22</sup> Such strong molecule–substrate interfacial interactions can force molecules to assemble into well-ordered structures controlled by the surface periodicity. In this article, we observe the formation of long-range ordered 2D pentacene:3,4,9,10-perylenetetracarboxylic dianhydride (PTCDA) supramolecular chiral networks on Ag(111) by low-temperature scanning tunneling microscopy (LT-STM). The 2D networks formed are controlled by interfacial interactions between molecules and interlocking with Ag(111) and are further stabilized through directional C=O···H–C multiple intermolecular H-bonding between PTCDA and pentacene.

## Experimental Section

The LT-STM experiments were carried out in a custom-built multichamber ultra-high-vacuum (UHV) system with base pressure better than  $6 \times 10^{-11}$  mbar, and housing an Omicron LT-STM interfaced to a Nanonis controller (Nanonis, Switzerland).<sup>23</sup> All STM imaging were performed at 77 K. A clean Ag(111) surface with large terraces was obtained after a few cycles of Ar<sup>+</sup> ion bombardment and subsequent annealing at 800 K. PTCDA (Sigma-Aldrich, 97%) and pentacene (Sigma-Aldrich, 99.9%, sublimed) were sequentially deposited by organic molecular beam deposition (OMBD) from two low-temperature Knudsen cells (MBE Komponenten, Germany) onto Ag(111) at room temperature in the growth chamber (base pressure  $< 2 \times 10^{-10}$  mbar).<sup>23a</sup> Prior to the deposition, PTCDA was purified twice by gradient vacuum sublimation (Creaphys, Germany). The deposition rates of pentacene and PTCDA were monitored by a quartz crystal microbalance (QCM) during evaporation and were further calibrated by counting the adsorbed molecule coverage in the large-scale LT-STM images at coverages below 1 monolayer (1 monolayer = one full monolayer of close-packed PTCDA or pentacene with their conjugated  $\pi$ -plane oriented parallel to the Ag surface). In our experiments, all depositions were performed at constant rates of about 0.015 ML/min for pentacene and 0.02 ML/min for PTCDA. During deposition, the chamber pressure was maintained below  $5.0 \times 10^{-10}$  mbar.

## Results and Discussion

Figure 1a shows a  $50 \times 50$  nm<sup>2</sup> STM image of a disordered pentacene:PTCDA mixed phase on Ag(111) at 77 K. Careful inspection of the STM image reveals that the surface is dominated by isolated but well-defined supramolecular nanostructures, comprising a PTCDA core surrounded by six pentacene molecules, where the center component with two bright and parallel stripes represents a PTCDA single molecule<sup>24,25</sup>

- (9) (a) Lin, N.; Dmitriev, A.; Weckesser, J.; Barth, J. V.; Kern, K. *Angew. Chem., Int. Ed.* **2002**, *41*, 4779. (b) Lingenfelder, M. A.; Spillmann, H.; Dmitriev, A.; Stepanow, S.; Lin, N.; Barth, J. V.; Kern, K. *Eur. J. Phys. Chem. B* **2006**, *110*, 23472. (d) Lin, N.; Stepanow, S.; Vidal, F.; Barth, J. V.; Kern, K. *Chem. Commun.* **2005**, 1681. (e) Spillmann, H.; Dmitriev, A.; Lin, N.; Messina, P.; Barth, J. V.; Kern, K. *J. Am. Chem. Soc.* **2003**, *125*, 10725. (f) Wang, Y.; Lingenfelder, M.; Classen, T.; Costantini, G.; Kern, K. *J. Am. Chem. Soc.* **2007**, *129*, 15742.
- (10) (a) Tahara, K.; Lei, S. B.; Mamdouh, W.; Yamaguchi, Y.; Ichikawa, T.; Uji-i, H.; Sonoda, M.; Hirose, K.; De Schryver, F. C.; De Feyter, S.; Tobe, Y. *J. Am. Chem. Soc.* **2008**, *130*, 6666. (b) Lei, S. B.; Tahara, K.; Feng, X. L.; Furukawa, S. H.; De Schryver, F. C.; Mullen, K.; Tobe, Y.; De Feyter, S. *J. Am. Chem. Soc.* **2008**, *130*, 7119. (c) Lei, S. B.; Tahara, K.; De Schryver, F. C.; Van der Auweraer, M.; Tobe, Y.; De Feyter, S. *Angew. Chem., Int. Ed.* **2008**, *47*, 2964.
- (11) (a) Zwanneveld, N. A. A.; Pawlak, R.; Abel, M.; Catalin, D.; Gigmes, D.; Bertin, D.; Porte, L. *J. Am. Chem. Soc.* **2008**, *130*, 6678. (b) Weigelt, S.; Busse, C.; Bombis, C.; Knudsen, M. M.; Goethel, K. V.; Strunskus, T.; Woll, C.; Dahlbom, M.; Hammer, B.; Laegsgaard, E.; Besenbacher, F.; Linderoth, T. R. *Angew. Chem., Int. Ed.* **2007**, *46*, 9227.
- (12) (a) Barlow, S. M.; Raval, R. *Surf. Sci. Rep.* **2003**, *50*, 201. (b) Humbolt, V.; Barlow, S. M.; Raval, R. *Prog. Surf. Sci.* **2004**, *76*, 1. (c) Xu, B.; Tao, C. G.; Cullen, W. G.; Reutt-Robey, J. E.; Williams, E. D. *Nano Lett.* **2005**, *5*, 2207. (d) Xu, B.; Tao, C. G.; Williams, E. D.; Reutt-Robey, J. E. *J. Am. Chem. Soc.* **2006**, *128*, 8493.
- (13) (a) Lorenzo, M. O.; Baddeley, C. J.; Muryn, C.; Raval, R. *Nature* **2000**, *404*, 376. (b) Kuhnle, A.; Linderoth, T. R.; Hammer, B.; Besenbacher, F. *Nature* **2002**, *415*, 891.
- (14) (a) Kuhnle, A.; Linderoth, T. R.; Besenbacher, F. *J. Am. Chem. Soc.* **2006**, *128*, 1076. (b) Greber, T.; Sljivancanin, Z.; Schillinger, R.; Wider, J.; Hammer, B. *Phys. Rev. Lett.* **2006**, *96*, 056103.
- (15) Bohringer, M.; Schneider, W. D.; Berndt, R. *Angew. Chem., Int. Ed.* **2000**, *39*, 792.
- (16) Chen, Q.; Richardson, N. V. *Nat. Mater.* **2003**, *2*, 324.
- (17) (a) Bohringer, M.; Morgenstern, K.; Schneider, W. D.; Berndt, R. *Angew. Chem., Int. Ed.* **1999**, *38*, 821. (b) Bohringer, M.; Morgenstern, K.; Schneider, W. D.; Berndt, R.; Mauri, F.; Vita, A.; De; Car, R. *Phys. Rev. Lett.* **1999**, *83*, 324.
- (18) Messina, P.; Dmitriev, A.; Lin, N.; Abel, M.; Spillmann, H.; Barth, J. V.; Kern, K. *J. Am. Chem. Soc.* **2002**, *124*, 14000.
- (19) (a) Fasel, R.; Parschau, M.; Ernst, K. H. *Nature* **2006**, *439*, 449. (b) Fasel, R.; Parschau, M.; Ernst, K. H. *Angew. Chem., Int. Ed.* **2003**, *42*, 5178.
- (20) Otero, R.; Lukas, M.; Kelly, R. E. A.; Xu, W.; Lagsgaard, E.; Stensgaard, I.; Kantorovich, L. N.; Besenbacher, F. *Science* **2008**, *319*, 312.
- (21) (a) Vonau, F.; Suhr, D.; Aubel, D.; Bouteiller, L.; Reiter, G.; Simon, L. *Phys. Rev. Lett.* **2005**, *94*, 066103. (b) Vonau, F.; Aubel, D.; Bouteiller, L.; Reiter, G.; Simon, L. *Phys. Rev. Lett.* **2007**, *99*, 086103.
- (22) (a) Lukas, S.; Witte, G.; Wöll, Ch. *Phys. Rev. Lett.* **2002**, *88*, 028301. (b) Yokoyama, T.; Takahashi, T.; Shinozaki, K. *Phys. Rev. Lett.* **2007**, *98*, 206102. (c) Fernandez-Torreto, I.; Monturet, S.; Franke, K. J.; Fraxedas, J.; Lorente, N.; Pascual, J. I. *Phys. Rev. Lett.* **2007**, *99*, 176103.
- (23) (a) Chen, W.; Huang, H.; Chen, S.; Chen, L.; Zhang, H. L.; Gao, X. Y.; Wee, A. T. S. *Appl. Phys. Lett.* **2007**, *91*, 114102. (b) Zhang, H. L.; Chen, W.; Chen, L.; Huang, H.; Wang, X. S.; Yuhsra, J.; Wee, A. T. S. *Small* **2007**, *3*, 2015. (c) Huang, H.; Chen, W.; Chen, L.; Zhang, H. L.; Wang, X. S.; Bao, S. N.; Wee, A. T. S. *Appl. Phys. Lett.* **2008**, *92*, 023105. (d) Chen, L.; Chen, W.; Huang, H.; Zhang, H. L.; Wee, A. T. S. *Adv. Mater.* **2008**, *20*, 484.
- (24) (a) Kraft, A.; Temirov, R.; Henze, S. K. M.; Soubatch, S.; Rohlfing, M.; Tautz, F. S. *Phys. Rev. B* **2006**, *74*, 041402. (b) Temirov, R.; Soubatch, S.; Luican, A.; Tautz, F. S. *Nature* **2006**, *444*, 350. (c) Tautz, F. S. *Prog. Surf. Sci.* **2007**, *82*, 479.
- (25) (a) Forrest, S. R. *Chem. Rev.* **1997**, *97*, 1793. (b) Zou, Y.; Kilian, L.; Schöll, A.; Schmidt, Th.; Fink, R.; Umbach, E. *Surf. Sci.* **2006**, *600*, 1240. (c) Glöckler, K.; Seidel, C.; Soukopp, A.; Sokolowski, M.; Umbach, E.; Börhringer, M.; Berndt, R.; Schneider, W.-D. *Surf. Sci.* **1998**, *405*, 1.

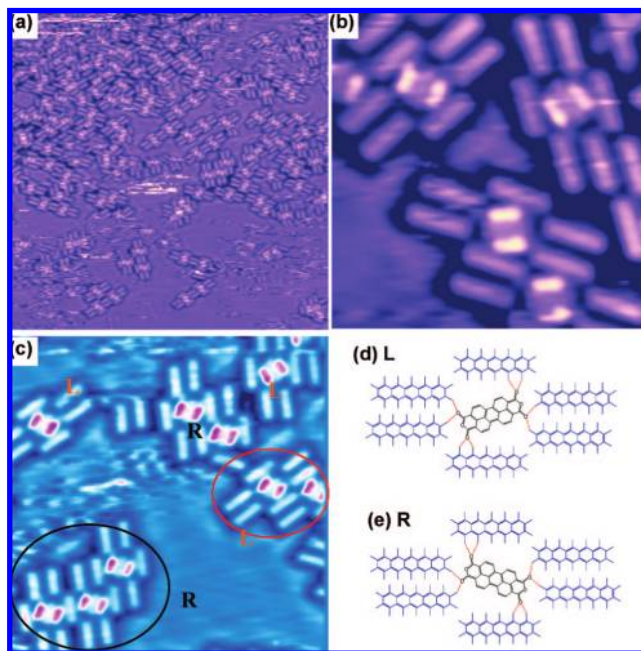


**Figure 1.** STM images of a disordered pentacene:PTCDA mixed phase consisting of the superstructures of a PTCDA core surrounded by six pentacene molecules on Ag(111). (a)  $50 \times 50 \text{ nm}^2$  and (b) corresponding detailed  $8 \times 8 \text{ nm}^2$  images. (c)  $14 \times 14 \text{ nm}^2$  STM image showing the coexistence of pentacene:PTCDA superstructures with L- and R-chirality. Their corresponding schematic drawings are shown in panels (d) and (e), where the dashed lines indicate the multiple in-plane intermolecular  $\text{C}=\text{O}\cdots\text{H}-\text{C}$  hydrogen-bonding between the PTCDA core and six surrounding pentacene molecules. ( $V_{\text{tip}} = 1.5 \text{ V}$  for panels a–c).

and the surrounding rodlike features are pentacene molecules.<sup>26</sup> This can be seen more clearly in the corresponding molecularly resolved  $8 \times 8 \text{ nm}^2$  STM image in Figure 1b. These pentacene:PTCDA nanostructures possess two in-plane mirror arrangements, i.e., surface chiral superstructures. They coexist on the surface, as highlighted by L- and R-assemblies in Figure 1(c). The schematic drawings of supramolecular arrangements of L- and R-assemblies are shown in Figure 1d and e, respectively.

During the STM imaging of the rather disordered pentacene:PTCDA mixed phase, we occasionally observed hopping of isolated pentacene:PTCDA superstructures on terraces at 77 K. For example, as shown in Figure 2a, there are two isolated pentacene:PTCDA assemblies (PTCDA core surrounded by a few pentacene molecules) at the lower-right corner. They diffused on the terrace toward the existing short-range ordered pentacene:PTCDA network and were immobilized there, as revealed by the STM image of the same area imaged 9 min later, shown in Figure 2b. Some of these diffused supramolecular assemblies maintain their original intermolecular bonding geometry during the hopping process. It is known that reversible and directional intermolecular H-bonding can lead to the formation of various surface supramolecular nanostructures or networks.<sup>5–7</sup> In particular, the intermolecular H-bonding between PTCDA anhydride groups and the aromatic hydrogen atoms of neighboring PTCDA gives rise to the formation of a well-defined herringbone arrangement of the PTCDA monolayer on Ag(111).<sup>24</sup> As such, we propose that the multiple in-plane

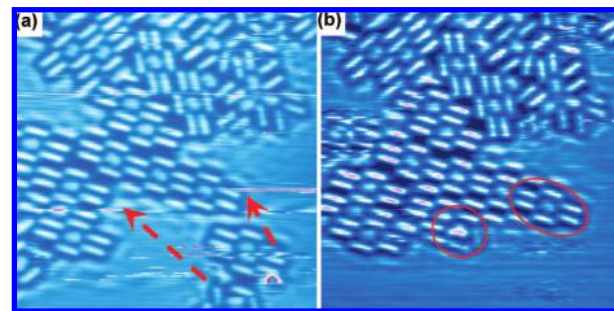


**Figure 2.** Sequential STM images ( $20 \times 20 \text{ nm}^2$ ,  $V_{\text{tip}} = -1.4 \text{ V}$ ) of a disordered pentacene:PTCDA mixed phase on Ag(111) showing the molecular diffusion: (a) origin image and (b) same area imaged 9 min later. The dashed arrows in panel (a) represent the molecular diffusion path, and circles in panel (b) highlight the two pentacene:PTCDA assemblies attached to the existing network.

intermolecular  $\text{C}=\text{O}\cdots\text{H}-\text{C}$  H-bonding between the anhydride groups of the PTCDA core and the peripheral aromatic hydrogen atoms of neighboring pentacene molecules plays an important role in stabilizing the pentacene:PTCDA superstructures. The possible  $\text{C}=\text{O}\cdots\text{H}-\text{C}$  H-bonding between PTCDA and pentacene is highlighted by dashed lines in Figure 1d,e.

The pentacene:PTCDA superstructures can extend on the Ag(111) terraces to form extended ordered surface networks. However, they are stable only above some critical size.<sup>20</sup> We observe the formation of the ordered pentacene:PTCDA supramolecular networks on Ag(111) after the sequential deposition of 0.7 ML of pentacene and 0.2 ML of PTCDA at room temperature. In contrast to the random mixing of L- and R-assemblies in the disordered pentacene:PTCDA mixed phase (Figure 1c), ordered surface networks are exclusively constructed from L- or R-assemblies and are referred to as L- or R-network as shown in the  $30 \times 30 \text{ nm}^2$  STM images in Figure 3a,c and their corresponding molecular resolved STM images in Figure 3b,d. Both networks are mirror domains with respect to each other. They adopt a p2 plane group with rectangular unit cell of  $a = 1.85 \pm 0.05 \text{ nm}$ ,  $b = 2.15 \pm 0.05 \text{ nm}$ , and  $\alpha = 90^\circ \pm 3^\circ$ , as highlighted in Figure 3b,d. The formation of 2D chiral pentacene:PTCDA networks arises from the cooperative arrangement of pentacene and PTCDA on Ag(111).

Self-organization of molecules into ordered nanostructures in extended surface networks relies on the interplay of multiple interactions on different strength and length scales.<sup>4–7,20–22</sup> In addition to the directional intermolecular interactions such as H-bonding, the formation of an extended supramolecular surface network usually requires strong molecule–substrate interfacial interactions, which can constrain molecules to adsorb in registry with the surface periodicity.<sup>21,22</sup> In this study, density functional theory (DFT) calculations and classic molecular dynamics (MD) simulations have been performed to rationalize the chiral conformations of the pentacene and PTCDA molecules adsorbed on Ag(111). We first study the interfacial interactions between isolated PTCDA or pentacene molecules and Ag(111) using plane-wave DFT calculations with the Vienna *ab initio* simulation package (VASP).<sup>27</sup> Ultrasoft pseudopotentials and the Perdew–Wang 1991 exchange-correlation functional in the VASP package were adopted.<sup>28</sup> The cutoff energy of the plane-

(26) (a) Repp, J.; Meyer, G.; Stojković, S. M.; Gourdon, A.; Joachim, C. *Phys. Rev. Lett.* **2005**, 94, 026803. (b) Zhang, H. L.; Chen, W.; Huang, H.; Chen, L.; Wee, A. T. S. *J. Am. Chem. Soc.* **2008**, 130, 2720.

(27) (a) Kresse, G.; Furthmüller, J. *Comput. Mater. Sci.* **1996**, 6, 15. (b) Kresse, G.; Furthmüller, J. *Phys. Rev. B* **1996**, 54, 11169.  
(28) Perdew, J. P.; Chevary, J. A.; Vosko, S. H.; Jackson, K. A.; Pederson, M. R.; Singh, D. J.; Fiolhais, C. *Phys. Rev. B* **1992**, 46, 6671.

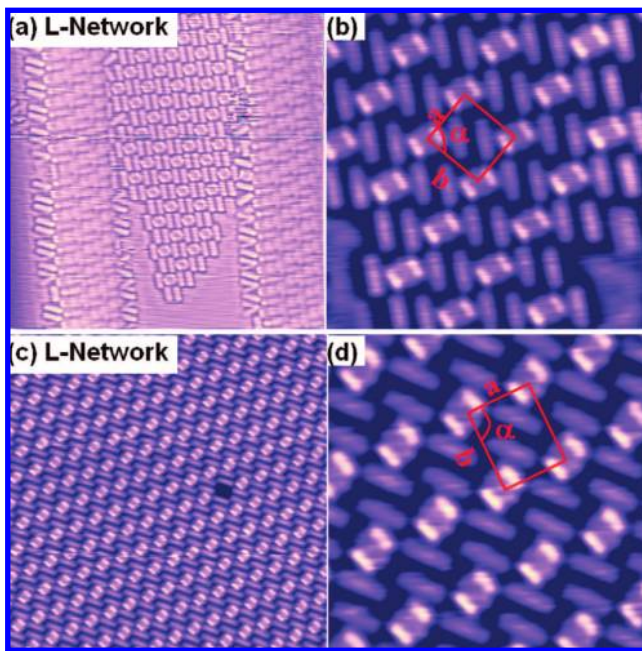


**Figure 3.** STM images of highly ordered pentacene:PTCDA 2D network with (a) L-chirality and (c) R-chirality ( $30 \times 30 \text{ nm}^2$ ,  $V_{\text{tip}} = 1.5 \text{ V}$ ), and their corresponding molecular resolved images in panels (b) and (d) ( $10 \times 10$  and  $8 \times 8 \text{ nm}^2$ , respectively). The rectangles in panels (b) and (d) highlight the unit cell with  $a = 1.85 \pm 0.05 \text{ nm}$ ,  $b = 2.15 \pm 0.05 \text{ nm}$ , and  $\alpha = 90^\circ \pm 3^\circ$ .

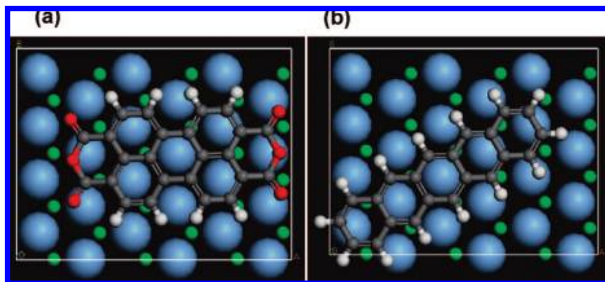


**Figure 4.** Optimized adsorption structures of (a) PTCDA and (b) pentacene on Ag(111) from DFT calculation using VASP.

wave was set at 400.0 eV. Two slab models, comprising  $3\sqrt{3} \times 3$  (18 Ag atoms per layer) and  $3\sqrt{3} \times 4$  (24 Ag atoms per layer) supercells with three and two repeating layers, respectively, were adopted. The adjacent slabs were separated by a vacuum layer of 10 Å. The large supercell ( $3\sqrt{3} \times 4$  model) allows pentacene or PTCDA molecules to form loosely packed structures, minimizing the effective intermolecular interaction. The structure optimizations were converged using the criterion of 20 meV/Å total force per atom.  $\mathbf{k}$ -point grids of  $2 \times 3 \times 1$  and  $2 \times 2 \times 1$  were used for summation over the surface Brillouin zone (SBZ), respectively. Both slab models yield nearly identical packing structures for pentacene or PTCDA on Ag(111), suggesting that the molecule–substrate interfacial interactions play a key role in determining the molecular adsorption structures. Figure 4 shows the optimized adsorption structures of PTCDA and pentacene on Ag(111) using the  $3\sqrt{3} \times 4$  supercell. Both pentacene and PTCDA molecules adopt the lying-down configuration with their conjugated  $\pi$ -plane parallel to Ag(111), arising from the effective coupling between

the  $\pi$ -electrons in molecules and the metal d-bands.<sup>29</sup> Clearly, C, H, and O atoms of both pentacene and PTCDA molecules predominantly adsorb at bridge or hollow sites of Ag(111), while the phenyl rings lie above the Ag atoms. The long molecular axis of pentacene orients approximately along the [110] direction of Ag(111), and that of PTCDA along the [1̄21] direction. The pentacene adsorbed on Ag(111) remains planar. PTCDA, on the other hand, adopts a distorted geometry with the anhydride groups bent toward to Ag(111) surface, consistent with previous theoretical results.<sup>30,31</sup> The preferential in-plane orientation of both molecules reveals an interlocking with Ag(111) surface atoms. Figures 1c and 2 show that, although there is no long-range order in the packing of pentacene:PTCDA superstructures, the long molecular axes of pentacene or PTCDA are rotated by multiples of 60° with respect to each other, coinciding with the three-fold symmetry of Ag(111). This implies a registry of adsorbed pentacene or PTCDA with Ag(111) and strong molecule–metal interfacial interactions. The Ag(111) substrate therefore acts as a template, constraining the lateral degrees of freedom of adsorbed PTCDA and pentacene molecules.

However, the formidable computational cost of the DFT method precludes its application to the coadsorption of both PTCDA and pentacene on Ag(111). The large adsorption distances between the adsorbed molecules and substrate preclude the possibility of chemical bond formation at the molecule–Ag(111) interfaces. In addition to the effective coupling between the metal d-bands and molecular  $\pi$ -electrons, the van der Waals-type interfacial dispersion force also plays a key role in determining the molecular adsorption on metal surfaces.<sup>32</sup> The low-cost force field method is hence a practical way to study the packing structures of both L and R pentacene:PTCDA 2D chiral networks on Ag(111). Classical force field models have already been demonstrated to give reasonable descriptions of stacking conformations of anthraquinone molecules on Cu(111),<sup>5d</sup> ionically functionalized polyacetylene sandwiched between Au electrodes,<sup>33a</sup> and molecular monolayer modified Si(111).<sup>33b</sup> Several models containing different numbers of adsorbed PTCDA and pentacene units, ranging from monomer to tetramer, were simulated using the consistent valence force field (CVFF) in the Materials Studio package.<sup>34</sup> The molecular ratio of pentacene vs PTCDA was selected according to the STM images. The Ag(111) surface model was large enough to allow the free motion of adsorbates. Consistent with LT-STM experiments, all trajectories were collected at 77 K in the production stage (duration of 100 ps). The adsorption sites for PTCDA and pentacene in the MD simulations are consistent with the optimized structures in DFT calculations, validating

- (29) (a) Chen, W.; Wang, L.; Qi, D. C.; Chen, S.; Gao, X. Y.; Wee, A. T. S. *Appl. Phys. Lett.* **2006**, 88, 184102. (b) Chen, W.; Huang, C.; Gao, X. Y.; Wang, L.; Zhen, C. G.; Qi, D. C.; Chen, S.; Zhang, H. L.; Loh, K. P.; Chen, Z. K.; Wee, W. T. S. *J. Phys. Chem. B* **2006**, 110, 26075. (c) Chen, W.; Chen, S.; Qi, D. C.; Gao, X. Y.; Chen, Z. K.; Wee, W. T. S. *Adv. Funct. Mater.* **2007**, 17, 1339.
- (30) (a) Hauschild, A.; Karki, K.; Cowie, B. C. C.; Rohlfing, M.; Tautz, F. S.; Sokolowski, M. *Phys. Rev. Lett.* **2005**, 94, 036106. (b) Hauschild, A.; Karki, K.; Cowie, B. C. C.; Rohlfing, M.; Tautz, F. S.; Sokolowski, M. *Phys. Rev. Lett.* **2005**, 95, 209602.
- (31) Du, S. X.; Gao, H. J.; Seidel, C.; Tsetseris, L.; Ji, W.; Kopf, H.; Chi, L. F.; Fuchs, H.; Pennycook, S. J.; Pantelides, S. T. *Phys. Rev. Lett.* **2006**, 97, 156105.
- (32) (a) Blankenburg, S.; Schmidt, W. G. *Phys. Rev. Lett.* **2007**, 99, 196107. (b) Blankenburg, S.; Schmidt, W. G. *Phys. Rev. B* **2006**, 74, 155419. (c) Preuss, M.; Schmidt, W. G.; Bechstedt, F. *Phys. Rev. Lett.* **2005**, 94, 236102.
- (33) (a) Cao, H.; Fang, T.; Li, S.; Ma, J. *Macromolecules* **2007**, 40, 4363. (b) Pei, Y.; Ma, J. *J. Am. Chem. Soc.* **2005**, 127, 6802.
- (34) *Materials Studio*, version 4.0; Accelrys Inc.: San Diego, 2006.

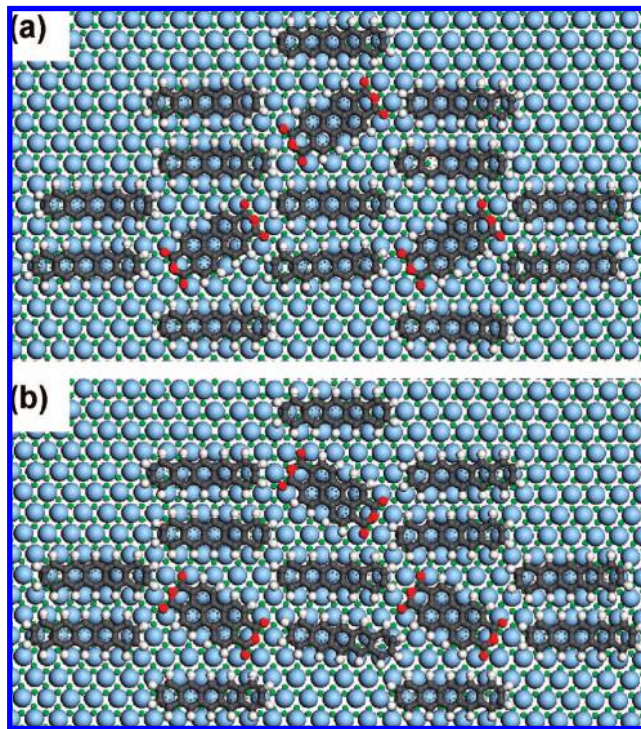


**Figure 5.** MD/CVFF simulation snapshots of pentacene:PTCDA 2D trimers with (a) L-chirality and (b) R-chirality.

the selected force field model in describing the adsorption of pentacene and PTCDA on Ag(111). Although the monomer (a PTCDA core surrounded by six pentacene molecules) shows some structural instability, the simulated superstructures of the dimer, trimer, and tetramer reproduce the observed pentacene:PTCDA supramolecular arrangements (Figures 13) with good structural rigidity at 77 K. Snapshots of simulated pentacene:PTCDA trimer superstructures are displayed in Figure 5: the simulated trimers also possess two mirror chiral arrangements, reproducing the L- and R-networks observed by LT-STM. Moreover, from MD simulations, C, H, and O atoms of both pentacene and PTCDA molecules prefer to adsorb at the bridge or hollow sites of Ag(111) and the phenyl rings directly above Ag atoms. This leads to the preferential in-plane stacking directions on Ag(111) with the long molecular axis of pentacene along [1̄10] and that of PTCDA along [1̄21], thereby suggesting a quasi-epitaxial interlocking with Ag(111). Hence, this force field simulation is consistent with our DFT calculation results shown in Figure 4. From the MD simulations, the H···O

distance (the distance between pentacene periphery hydrogen atoms and the oxygen atoms of PTCDA anhydride groups) in the stabilized dimer, trimer, and tetramer is  $\sim$ 2.6–2.7 Å, reflecting weak hydrogen-bonding.<sup>35,36</sup> Our LT-STM experiments and DFT calculations reveal that the formation of 2D pentacene:PTCDA supramolecular chiral networks on Ag(111) is controlled by the strong molecule–substrate interfacial interactions and is further stabilized through multiple in-plane intermolecular H-bonds between the PTCDA core and the neighboring pentacene molecules.

### Conclusion

We report the formation of well-ordered 2D pentacene:PTCDA supramolecular chiral networks through the cooperative arrangement of pentacene and PTCDA on Ag(111), as revealed by LT-STM studies. Our DFT and MD results reveal a registry of adsorbed pentacene or PTCDA with the underlying Ag(111). This suggests that the adsorption of pentacene or PTCDA on Ag(111) involves a strong molecule–substrate interfacial interaction, which plays a key role in determining the formation of the 2D pentacene:PTCDA supramolecular chiral networks. Ag(111) acts as a template to restrict the lateral degrees of freedom of the adsorbed pentacene and PTCDA molecules and locks them into specific adsorption sites due to the corrugation of the potential energy surface,<sup>32</sup> thereby favoring the formation of well-ordered 2D pentacene:PTCDA chiral networks. The skeleton of the pentacene:PTCDA networks is further strengthened through multiple in-plane intermolecular C=O···H–C H-bonds between the anhydride groups of the PTCDA core and the aromatic hydrogen atoms of the neighboring pentacene molecules. Our results suggest that the formation of large-scale, highly periodic 2D supramolecular assemblies often relies on a combination of specific and relatively strong molecule–substrate interactions with weak but directional intermolecular interactions.

**Acknowledgment.** W.C. acknowledges financial support from a LKY PDF fellowship. The authors acknowledge support from Singapore A\*STAR grant R-398-000-036-305, ARF grant R-144-000-196-112, and China NSF under nos. 20573050 and 20433020.

JA801577Z

- (35) (a) Steiner, T. *Angew. Chem., Int. Ed.* **2002**, *41*, 48. (b) Espinosa, E.; Molins, E.; Leconte, C. *Chem. Phys. Lett.* **1998**, *285*, 170.  
 (36) (a) Abel, M.; Oison, V.; Koudia, M.; Maurel, C.; Katan, C.; Porte, L. *ChemPhysChem* **2006**, *7*, 82. (b) Koudia, M.; Abel, M.; Maurel, C.; Bliek, A.; Catalin, D.; Mossoyan, M.; Mossoyan, J. C.; Porte, L. *J. Phys. Chem. B* **2006**, *110*, 10058. (c) Oison, V.; Koudia, M.; Abel, M.; Porte, L. *Phys. Rev. B* **2007**, *75*, 035428. (d) Barrena, E.; de Oteyza, D. G.; Dosch, H.; Wakayama, Y. *ChemPhysChem* **2007**, *8*, 1915.